Journal of Hydrology 555 (2017) 724–735

Contents lists available at ScienceDirect

Journal of Hydrology

journal homepage: www.elsevier.com/locate/jhydrol

Research papers

Transport and fate of viruses in sediment and stormwater from a Managed Aquifer Recharge site

Salini Sasidharan [a,b,c,d,e,*], Scott A. Bradford [d], Jiří Šimůnek [e], Saeed Torkzaban [c], Joanne Vanderzalm [a]

[a] CSIRO Land and Water, Glen Osmond, SA 5064, Australia
[b] National Centre for Groundwater Research and Training, SA 5001, Australia
[c] Flinders University, Adelaide, SA 5001, Australia
[d] USDA, ARS, Salinity Laboratory, Riverside, CA 92507, United States
[e] Department of Environmental Sciences, University of California, Riverside, CA 92507, United States

ARTICLE INFO

Article history:
Received 16 August 2017
Received in revised form 14 October 2017
Accepted 25 October 2017
Available online 27 October 2017
This manuscript was handled by Prof. P. Kitanidis, Editor-in-Chief, with the assistance of Martin Thullner, Associate Editor

Keywords:
Virus
Calcium
Transport
Solid phase inactivation
Stormwater
Managed Aquifer Recharge

ABSTRACT

Enteric viruses are one of the major concerns in water reclamation and reuse at Managed Aquifer Recharge (MAR) sites. In this study, the transport and fate of bacteriophages MS2, PRD1, and ΦX174 were studied in sediment and stormwater (SW) collected from a MAR site in Parafield, Australia. Column experiments were conducted using SW, stormwater in equilibrium with the aquifer sediment (EQ-SW), and two pore-water velocities (1 and 5 m day^{-1}) to encompass expected behavior at the MAR site. The aquifer sediment removed >92.3% of these viruses under all of the considered MAR conditions. However, much greater virus removal (4.6 logs) occurred at the lower pore-water velocity and in EQ-SW that had a higher ionic strength and Ca^{2+} concentration. Virus removal was greatest for MS2, followed by PRD1, and then ΦX174 for a given physicochemical condition. The vast majority of the attached viruses were irreversibly attached or inactivated on the solid phase, and injection of Milli-Q water or beef extract at pH = 10 only mobilized a small fraction of attached viruses (<0.64%). Virus breakthrough curves (BTCs) were successfully simulated using an advective–dispersive model that accounted for rates of attachment (k_{att}), detachment (k_{det}), irreversible attachment or solid phase inactivation (μ_s), and blocking. Existing MAR guidelines only consider the removal of viruses via liquid phase inactivation (μ_l). However, our results indicated that $k_{att} > \mu_s > k_{det} > \mu_l$, and k_{att} was several orders of magnitude greater than μ_l. Therefore, current microbial risk assessment methods in the MAR guideline may be overly conservative in some instances. Interestingly, virus BTCs exhibited blocking behavior and the calculated solid surface area that contributed to the attachment was very small. Additional research is therefore warranted to study the potential influence of blocking on virus transport and potential implications for MAR guidelines.

1. Introduction

The availability of high-quality drinking water has decreased due to climate variability and population growth, while demand has increased to meet agricultural, industrial, environmental, and municipal water needs (Levantesi et al., 2010; Shannon et al., 2008; Yates et al., 1987). The United Nations has estimated that about 1.8 billion people around the globe will face severe water stress and scarcity by 2025 (UN, 2013). Consequently, there is an urgent need to find alternative sources of freshwater, such as by developing economic and effective water reclamation, recycling, and preservation techniques (Levantesi et al., 2010; Shannon et al., 2008; Yates et al., 1987). Water recycling can be achieved by various engineering techniques and natural or passive treatment. Major water recycling techniques employ multiple barrier approaches, including secondary treatment, riverbank filtration, reverse osmosis, UV disinfection, chlorination, and ultrafiltration (Page et al., 2010a). However, many countries across the world do not have access to cheap and efficient wastewater treatment plants (Vega et al., 2003). Managed Aquifer Recharge (MAR) is a collection of natural treatment techniques, including Aquifer Storage, Transfer, and Recovery (ASTR) or Aquifer Storage and Recovery (ASR), that has gained a lot of attention recently (Ayuso-Gabella et al., 2011; Bekele et al., 2014, 2013, 2011; Stevens, 2014; Toze and Bekele, 2009; Ward and Dillon, 2009). Water recycling is facilitated during MAR by purposefully recharging lower quality water into aquifers for natural treatment prior to recovery (Dillon et al., 2009; Page et al., 2010a). Currently, MAR is considered as an effec-

* Corresponding author at: USDA, ARS, Salinity Laboratory, Riverside, CA 92507, United States.
E-mail address: salinis@ucr.edu (S. Sasidharan).

https://doi.org/10.1016/j.jhydrol.2017.10.062
0022-1694/

tive and economical option to store water in the treatment train; e.g., a sequence of multiple stormwater treatments, which are designed to meet the needs of a particular environment, in order to maximize results (MelbourneWater, 2017). MAR provides a natural buffer, increases public perception, provides a residence time that can facilitate removal of biodegradable organic matter and pathogens, improves the quality of the treated wastewater or stormwater, and reduces the cost of seasonal peak demands (Dillon et al., 2009; Levantesi et al., 2010; Page et al., 2010a; Page et al., 2010c). However, current MAR guidelines require expensive and energy-intensive pre-treatment of injected water and post-treatment of recovered water depending on the end use, with drinking water supply requiring the highest level of treatment (Dillon et al., 2009).

One of the major concerns with potable water reuse is the microbiological quality of recovered water and the possibility of transmitting infectious diseases from pathogenic microorganisms (virus, bacteria, and protozoa) that are not eliminated by conventional wastewater treatment (Costán-Longares et al., 2008; Levantesi et al., 2010; Shannon et al., 2008). Enteric viruses pose the greatest public health concern because they can travel long distances (Schijven and Hassanizadeh, 2000) and are infectious at very low doses (Ward et al., 1986). MAR systems can improve the microbiological quality of water by natural attenuation processes during soil filtration and/or aquifer transport (Asano et al., 2007; Dillon et al., 2008; Levantesi et al., 2010; Mayotte et al., 2017). For example, inactivation occurs when viruses lose their ability to infect host cells and replicate because of the disruption of proteins and the degradation of nucleic acid (Gerba, 1984; Schijven et al., 2003). The most important factors affecting virus inactivation rate include temperature, groundwater microbial activity, pH, salt species and concentration, some forms of organic matter, and virus type (McCarthy and McKay, 2004; Schijven and Hassanizadeh, 2000). However, decay rates for human enteric viruses, determined using diffusion chambers in monitoring wells at MAR sites, have been found to be slow and nonlinear (Sidhu et al., 2015; Sidhu and Toze, 2012). Quantitative microbial risk assessment calculations for MAR systems have been developed from a detailed hydrogeological assessment of the aquifer and in-situ decay studies (Donald et al., 2011; Page et al., 2010b, 2015a; Toze et al., 2010). These risk assessment studies considered that liquid phase virus inactivation was the only reliable mechanism for virus removal in the aquifer, and neglected the processes of virus attachment, detachment, and solid phase inactivation (Abu-Ashour et al. (1994); Dillon et al., 2008).

In addition to liquid phase inactivation, virus removal from groundwater may occur by attachment from the bulk solution to the solid phase (Shen et al., 2012a,b), whereas detachment refers to the reverse process of virus release from the solid phase to the bulk solution (Bergendahl and Grasso, 2000). Virus attachment to aquifer materials is a strong function of many physicochemical variables, including pore-water velocity (Hijnen et al., 2005); solution ionic strength (IS) (Da Silva et al., 2011; Knappett et al., 2008; Xu et al., 2005); solution ionic composition (Bales et al., 1991; Lipson and Stotzky, 1983; Sadeghi et al., 2013; Sasidharan et al., 2014; Walshe et al., 2010); and the presence of humic materials (Zhuang and Jin, 2003), and metal oxides (Foppen et al., 2006). Consequently, an accurate assessment of virus attachment at MAR sites must consider realistic solution chemistries and aquifer mineralogy. In contrast, most virus transport studies have been conducted under highly idealized conditions using clean sand or glass beads, and simple electrolyte solutions.

Attachment during MAR can only serve as an effective, long-term treatment when viruses are irreversibly retained or inactivated on the solid phase. It is difficult to separately quantify the processes of irreversible attachment and solid phase inactivation because they both decrease the number of infective viruses that can detach from the solid phase (Ryan et al., 2002). Consequently, much less is known about solid than liquid phase inactivation (Murray and Laband, 1979; Ryan et al., 2002). Solid phase inactivation has been reported to increase with the strength of the adhesive interaction and the temperature (Loveland et al., 1996; Murray and Laband, 1979; Ryan et al., 2002). Yates et al. (1985) found that the inactivation rate of MS2 in eleven groundwater samples increased with the Ca^{2+} concentration. However, low levels of virus detachment have been commonly observed under steady-state physicochemical conditions (Bales et al., 1993). Furthermore, changes in solution chemistry (e.g., a decrease in IS or an increase in pH) have been observed to produce large pulses of released colloids (Bales et al., 1993). Consequently, there is a concern that attached viruses can be remobilized with a decrease in IS or divalent cation concentrations during rainfall events (Gerba, 1983; Yates et al., 1988).

The main objective of this work was to systematically examine virus removal processes in urban stormwater from a wetland (Urrbrae, South Australia) when in contact with aquifer sediment collected from an ASTR site (Parafield Gardens, South Australia). Three bacteriophages (PRD1, MS2, and ΦX174) were used as surrogate viruses for enteric human viruses. Laboratory scale virus transport experiments and inactivation studies were conducted. Additional studies investigated the release of attached viruses by sequentially injecting step pulses of solutions with alternating solution chemistry. Virus breakthrough curves (BTCs) were simulated using the numerical solution of the advection–dispersion equation with terms for attachment, detachment, Langmuirian blocking, and a sink term that accounted for irreversible attachment and solid phase inactivation. Model parameters were obtained by inverse fitting to the observed BTCs. Results from this study provide valuable insight on the relative importance of natural attenuation processes for viruses at MAR sites and indicate that microbial risk assessments that only consider liquid phase inactivation may be overly conservative in some instances.

2. Materials and methods

2.1. Stormwater

Stormwater (SW) samples were collected from the Urrbrae Wetland located in Mitcham, South Australia (Fig. S1). The wetlands were constructed to collect urban stormwater for flood protection in the nearby area and for potential future use in MAR operations (Lin et al., 2006). The stormwater chemistry (major and minor elements) was analyzed using an Inductively Coupled Plasma Mass Spectrometry (ICP-MS) and the carbon content was measured using Varo TOC Cube (Analytical Chemistry, CSIRO, Adelaide). The pH and electrical conductivity (EC) were measured using a Eutech PC 700 (Eutech Instruments).

Dissolved calcium is a weathering product of almost all rocks and is, consequently, abundant in most groundwater sources. Water from limestone aquifers may contain 30–100 mg L^{-1} of calcium, gypsiferous shale aquifers may contain several hundred milligrams per liter (Sadeghi et al., 2013), and dolomite produces water with high levels of calcium and magnesium (Wade, 1992). The calcium concentrations range from 0.03 to 36.5 mg L^{-1} in Australian groundwaters (Radke et al., 1998). When water percolates through soils, the concentration of divalent cations in soil solutions often increases with depth along the vertical weathering-leaching gradient (Sadeghi et al., 2013; Sverdrup and Warfvinge, 1993). It is, therefore, logical to anticipate that the solution IS and divalent cation concentration will increase with a travel distance and residence time during ASTR, due to mineral dissolution, along with

mixing in aquifers containing groundwater of higher salinity. In a limestone aquifer, increases in calcium are prevalent due to the dissolution of calcium carbonate. This increase in solution IS and Ca^{2+} concentration may increase virus attachment. Virus transport and survival experiments were therefore also conducted using stormwater after it was equilibrated with the aquifer sediment (50 g of sediment with 200 mL of stormwater), denoted as EQ-SW. Table S1 provides a summary of selected chemical properties for EQ-SW.

2.2. Porous media

Aquifer materials were collected from an ASTR site situated in Parafield Gardens, Adelaide, Australia (Fig. S1) established for stormwater storage and treatment (Page et al., 2015b). The target aquifer for ASTR is the lower Tertiary marine sediments of the Port Willunga Formation (T2 aquifer), a well-cemented sandy limestone aquifer which is intersected between −149 and −214 m Australian Height Datum (AHD) (160–220 m below ground surface). At this location, the target aquifer is approximately 60 m thick and overlain by 7 m thick clay aquitard of Munno Para Clay which prevents the migration of injected stormwater to the overlying aquifers. A schematic cross-section of the aquifer is given in Fig. S2. Karstic features were not identified during construction of the site (Vanderzalm et al., 2010). The mineralogy in the storage zone is dominated by calcite (65 ± 23%), quartz (30 ± 22%), and a trace amount of ankerite, goethite, hematite, pyrite, albite, and microcline (Vanderzalm et al., 2010). Goethite and hematite largely account for the 2.1% Fe_2O_3 quantified by X-ray Fluorescence (XRF). The transmissivity of the aquifer ranges from 100 to >200 $m^2\ d^{-1}$, depending on the silt content and degree of weathering (Miotliński et al., 2014). Considerable variability exists in hydraulic conductivity within the aquifer and, therefore, the ASTR was constructed with partially penetrating wells to avoid the zone of high hydraulic conductivity in the lower part of the aquifer and to exclude excessive mixing between native groundwater and injection water (Miotliński et al., 2014). The aquifer is low in organic carbon (<0.5%) and has an average cation exchange capacity of 1.5 meq/100 g (Page et al., 2010b). The aquifer has a temperature of 25 °C at ambient conditions. The design, operation, hydraulic, chemical, and physical properties of this aquifer has been extensively studied and reported in the literature (Adkinson et al., 2008; Dillon et al., 2008; Kremer et al., 2008; Page et al., 2010b; Pavelic et al., 2004; Rinck-Pfeiffer et al., 2005; Vanderzalm et al., 2010). The aquifer material used in this study was obtained from intact core samples taken at a depth of 171.30 m below the ground surface. The collected aquifer sediments were directly used in the experiments without any further treatment. Selected physical and chemical properties of the sediment are provided in Table S2. The bulk mineralogy of the sediment sample was determined by X-ray Diffraction (XRD). The major elemental composition was determined by XRF and Inductively Coupled Plasma Optical Emission Spectrometry (ICP-OES) following reverse aqua regia acid digest. Sieve analysis was used to determine the particle size distribution.

Additional transport experiments were conducted using ultra-pure clean quartz sand (Charles B. Chrystal CO., Inc., NY, USA) with size ranging from 125 to 300 μm. This sand was cleaned using an acid wash and boiling procedure described by Sasidharan et al. (2014). Transport experiments with the ultra-pure quartz sand represent a worst-case scenario for virus transport because of minimal chemical heterogeneity.

2.3. Viruses

Bacteriophage MS2, PRD1, and ΦX174 were used as model viruses in this study. These microbes were chosen because of their structural resemblance to many human enteric viruses and they have been used in numerous investigations as surrogates for human enteric viruses (Chu et al., 2003; Schijven and Hassanizadeh, 2000). It should be mentioned that recent studies have demonstrated that the transport and fate of human enteric viruses may not always be well correlated with that of bacteriophages (Bellou et al., 2015). Additional research is, therefore, warranted to identify the best surrogate for the transport and fate of pathogenic viruses, but this issue is beyond the scope of the present study. The bacteriophages were analyzed using their respective *Escherichia coli* host. The production of bacteriophages and their analysis using double layer agar (DLA) methods were detailed in Sasidharan et al. (2016). Stock solutions of viruses were diluted in stormwater to obtain an initial concentration (C_0) of $\sim 5 \times 10^6$ plaque forming unit mL^{-1}. The survival of viruses over a 7 h interval was determined in both SW and EQ-SW solutions.

2.4. Zeta potential and size measurements

The electrophoretic mobility (EM) of viruses, crushed aquifer sediment, and quartz (<2 μm) was measured in both SW and EQ-SW using a Zetasizer (Malvern, Zetasizer Nano Series, Nano-ZS). The EM measurements were repeated five times with more than twenty runs per measurement. The Smoluchowski equation (Elimelech et al., 1994) was used to convert the measured EM values to zeta potentials. The size distribution of viruses in both SW and EQ-SW was measured using a dynamic light scattering (DLS) (Malvern Instruments Ltd, 2004; Sikora et al., 2016) process (Malvern, Zetasizer Nano Series, Nano-ZS).

2.5. Transport experiments

The column experiments were set up in a constant temperature laboratory (20 °C). Sterilized polycarbonate columns (1.9 cm inside diameter and 11 cm height) were wet packed using aquifer material or ultra-pure quartz sand while the column was being vibrated. After packing, the column was preconditioned with >10 pore volumes (PV) of stormwater water using a syringe pump (Model 22, Harvard Apparatus) at a flow rate of 0.394 mL min^{-1}. A suspension with known C_0 of viruses (PRD1, MS2, and ΦX174) and solution chemistry (SW or EQ-SW) was introduced into the column using a syringe pump at a constant pore water velocity (1 or 5 m day^{-1}) for 13 PV (Phase I), followed by injection of ~7 PV of virus-free solution at the same solution chemistry and velocity (Phase II). To study the reversibility of attached viruses, the experiments were continued by flushing the columns with ~11 PV of Milli-Q water (Phase III), followed by injection of 3% Beef Extract with pH = 10 (Phase IV). Virus release is enhanced in Milli-Q water by a reduction in solution IS which expands the double layer thickness, and increases the magnitude of the sediment and virus zeta potentials (Chen et al., 2014; Sasidharan et al., 2017b). Beef extract is a mixture of peptides, amino acids, nucleotide fractions, organic acids, minerals, and some vitamins, with a pH of 10 and its injection further enhances the virus release by masking positively charged sites with organic matter, and reversing the charge of some pH dependent sites (Landry et al., 1978; McMinn, 2013). Effluent samples were collected using a fraction collector (CF-2, Spectrum, USA). The effluent concentrations (C) of viruses were enumerated using the methods described above. Separate column experiments were run for each porous medium (aquifer sediment or ultra-pure quartz sand), solution chemistry (SW or EQ-SW), and pore-water velocity (1 or 5 m day^{-1}) combination.

Breakthrough curves (BTCs) were plotted as a dimensionless concentration (C/C_0) of viruses as a function of PVs. A mass balance was conducted for the viruses in the column experiments using information on injected and recovered viruses during Phases I–

IV. The percentage of virus mass retained on the solid phase (M_s) was determined as the difference in the mass of injected virus and mass of virus recovered in the effluent BTC ($MBTC = M_I + M_{II}$) during Phases I and II. The percentage of injected viruses that was recovered during Phases III and IV were denoted as M_{III} and M_{IV}, respectively. The percentage of injected viruses that were irreversibly retained (M_{irr}) was determined as 100-$MBTC$-M_{III}-M_{IV}. The log removal of the viruses in the column effluent experiments was determined as $-\log_{10}(M_{BTC})$.

2.6. Simulation of virus BTCs

Experimental BTCs for viruses were simulated using the HYDRUS-1D model (Šimůnek et al., 2016). The HYDRUS-1D program numerically solves the Richards' equation for variably saturated water flow and Fickian-based advection–dispersion equations for heat and solute transport. The governing continuum-scale flow and transport equations are solved numerically using Galerkin-type linear finite element schemes (Šimůnek et al., 2016). The following aqueous and solid phase mass balance equations were considered in this model for each virus.

$$\frac{\partial C}{\partial t} = \lambda v \frac{\partial^2 C}{\partial z^2} - v\frac{\partial C}{\partial z} - k_{att}\psi C - k_{det}\frac{\rho_b}{\theta}S - \mu_l C \quad (1)$$

$$\frac{\rho_b}{\theta}\frac{\partial S}{\partial t} = k_{att}\psi C - k_{det}\frac{\rho_b}{\theta}S - \mu_s\frac{\rho_b}{\theta}S \quad (2)$$

where t (T; T denotes unit of time) is time, z (L; L denotes units of length) is the direction of mean water flow, C (NL^{-3}; N denotes the virus number) is the aqueous phase virus concentration, λ (L) is the dispersivity, v (LT^{-1}) is the average pore water velocity, ρ_b (ML^{-3}; M denotes the unit of mass) is the bulk density, θ is the water content, S (NM^{-1}) is the solid phase concentrations of virus, k_{att} (T^{-1}) is the virus attachment rate coefficient, k_{det} (T^{-1}) is the virus detachment rate coefficient, and μ_s (T^{-1}) is a sink term which accounts for irreversible attachment and inactivation of viruses attached on the solid phase, and μ_l (T^{-1}) is the inactivation rate coefficient for viruses in the liquid phase. The parameter ψ is a dimensionless Langmuirian blocking function that is given as (Adamczyk et al., 1994)

$$\psi = \left(1 - \frac{S}{S_{max}}\right) \quad (3)$$

where S_{max} (NM^{-1}) is the maximum solid phase concentrations of retained virus.

The fraction of the solid surface area that is available for retention (S_f) was calculated from S_{max} as (Kim et al., 2009; Sasidharan et al., 2014):

$$S_f = \frac{A_c \rho_b S_{max}}{(1-\gamma)A_s} \quad (4)$$

where A_c (L^2N^{-1}) is the cross sectional area of a virus, A_s (L^{-1}) is the solid surface geometric area per unit volume, and γ is the porosity of a monolayer packing of viruses on the solid surface that was taken from the literature to be 0.5 (Johnson and Elimelech, 1995).

The value of the sticking efficiency (α) was determined from the fitted k_{att} value and the filtration theory as (Schijven and Hassanizadeh, 2000; Yao et al., 1971):

$$\alpha = \frac{2d_c k_{att}}{3(1-n)v\eta} \quad (5)$$

where n is the porosity (0.4) and d_c (L) is the collector (median grain) diameter. The value of the single collector-efficiency, η, was calculated using the correlation equation presented by (Messina et al., 2015).

3. Results and discussion

3.1. Characterization of solution chemistry

SW had a pH of 7 and EC of 260 μS cm^{-1} and after equilibration with the aquifer sediment the pH and EC of the EQ-SW increased to 7.3 and 2230 μS cm^{-1}, respectively (Table S1). In addition, the concentration of all major ions also increased in EQ-SW, notably, with ~7 times increase in Ca and K, and ~11 times increase in Na concentration. Therefore, the ionic strength of the EQ-SW (0.014 mM) increased 10 times compared to SW (0.002 mM). This increase in pH and EC of EQ-SW compared to SW was attributed to the dissolution of limestone in the aquifer sediment (Table S2) that leaches $CaCO_3$ and increases the solution pH (Earle, 2013; Panthi, 2003). The measured concentration value of Ca^{2+} in EQ-SW (151 mg L^{-1}, Table S1) was very close to Ca^{2+} (135 ± 5 mg L^{-1}) in ambient groundwater from the T2 aquifer (Page et al., 2010b) and, therefore, it confirms that the solution chemistry of the EQ-SW was representative of the target aquifer.

3.2. Characterization of aquifer sediment

The average particle size of the sediment was ~110 μm, with 93.5% within the 20–200 μm size fraction (Table S2) and only 6.5% in smaller or larger size fractions. The quantitative bulk mineralogy of the sediment in Table S2 showed that the aquifer material was made of quartz (58.1%), calcite (35.0%), and goethite (2.2%). Major element analysis (Table S2) indicates the presence of a large fraction of SiO_2 (53.4%), Al_2O_3 (1.2%), Fe_2O_3 (3.5%), and CaO (19.6%). Acid digest data (Table S2) revealed the presence of other major ions such as K, Mg, and Na in the sediment. These results demonstrated that the sediment was rich in major metal oxides such as CaO, MgO, Fe_2O_3, and Al_2O_3, as well as minerals such as quartz and clays. The metal oxide surfaces are positively charged and the mineral surfaces are negatively charged at the experimental pH (~7.3) due to surface chemical reactions with H^+/OH^- ions, respectively (Tombácz, 2009). Consequently, the aquifer sediment surface is expected to be chemically heterogeneous and possess a distribution of negative and positive surface charges. It has been shown that minor degrees of positive charge heterogeneity on the collector surface result in attachment rates that are an order of magnitude larger than similar surfaces having no charge heterogeneity (Schijven and Hassanizadeh, 2000).

Table 1 shows that the crushed aquifer sediment and quartz were negatively charged in the presence of SW and EQ-SW. We assume that some of the positively charged surfaces were masked

Table 1
The measured zeta potential values of viruses and sediment and the measured values of the size of viruses in stormwater (SW) and stormwater equilibrated with aquifer sediment (EQ-SW).

Virus	Solution	ζ+ [mV]	Size [nm]
MS2	SW	−22.4 ± 1.2	27.6 ± 3.4
	EQ-SW	−12.6 ± 1.1	28.3 ± 3.3
ΦX174	SW	−23.8 ± 1.2	29.6 ± 2.6
	EQ-SW	−13.7 ± 0.9	30.0 ± 2.9
PRD1	SW	−23.3 ± 1.4	69.0 ± 0.82
	EQ-SW	−14.8 ± 1.3	68.3 ± 2.5
Sediment	SW	−19.8 ± 0.8	–
	EQ-SW	−16.2 ± 1.5	–
Quartz	SW	−31.5 ± 2.8	–
	EQ-SW	−27.2 ± 1.3	–

by negatively charged P, Dissolved Organic Carbon (DOC), and Dissolved Inorganic Carbon (DIC) present in the SW (Table S1), which will lead to a reduction in the overall surface potential and a net negative zeta potential value for the sediment (ζ_{sand}^{-}) (Karageorgiou et al., 2007). Furthermore, the presence of SiO_2 and clays will significantly decrease the value of ζ_{sand}^{-} (Chen et al., 2014). Consequently, the zeta potential for quartz was lower than the aquifer sediment (Table 1). Table 1 also indicates that the zeta potential for the aquifer sediment and quartz was more negatively charged in the presence of SW than EQ-SW. This could be explained by an increase in EC, divalent cation (Ca^{2+} and Mg^{2+}) concentration, and IS by more than 8 times in EQ-SW compared to SW, and the compression of the electrostatic double layer (Elimelech, 1994). Increased Ca^{2+} concentration can also lead to charge reversal (Lipson and Stotzky, 1983; Moore et al., 1981; Redman et al., 1999; Roy and Dzombak, 1996) and charge neutralization (Bales et al., 1991).

3.3. Characterization of viruses

The average size of MS2, ΦX174, and PRD1 was measured to be 27.6–28.3 nm, 29.6–30.0 nm, and 68.0–69.0 nm, respectively. These values are within 3–5 nm of previously reported values (Chrysikopoulos and Aravantinou, 2012; Sasidharan et al., 2016; Thomson, 2005), and this indicates that aggregation of these viruses was negligible under our experimental solution chemistry conditions. Table 1 shows the measured zeta potential values of viruses in SW and EQ-SW. The absolute value of the zeta potential for these viruses was always negative, but smaller in magnitude in the presence of EQ-SW compared to SW. Similar to the sediment, this can be explained by an increase in IS, compression of the double layer, and higher Ca^{2+} concentration for EQ-SW. In addition, Ca^{2+} is expected to bind to the carboxyl functional groups on the viral protein capsid which reduces the negative surface charge density (Harvey and Ryan, 2004).

3.4. Virus retention under various physicochemical conditions

Fig. 1 shows observed and fitted BTCs for the viruses under various solution chemistry (SW and EQ-SW) and pore-water velocity (1 and 5 m day^{-1}) conditions. The normalized effluent concentrations C/C_0 (where C_0 is the influent and C is the effluent virus concentration) were plotted as a function of pore volumes. Table 2 presents experimental mass balance (M_{BTC}, M_s, M_{III}, M_{IV}, and M_{irr}) information. This data is summarized in Fig. 2 which presents bar plots of the log removal (e.g., $-\log_{10}(M_{BTC})$) of viruses under different physicochemical conditions. The value of M_s = 26.2% is in the worst-case transport scenario using clean quartz sand and SW at 5 m day^{-1} (Fig. S3). In contrast, values of M_s in the aquifer sediment were always much higher (>92.3%) than this control

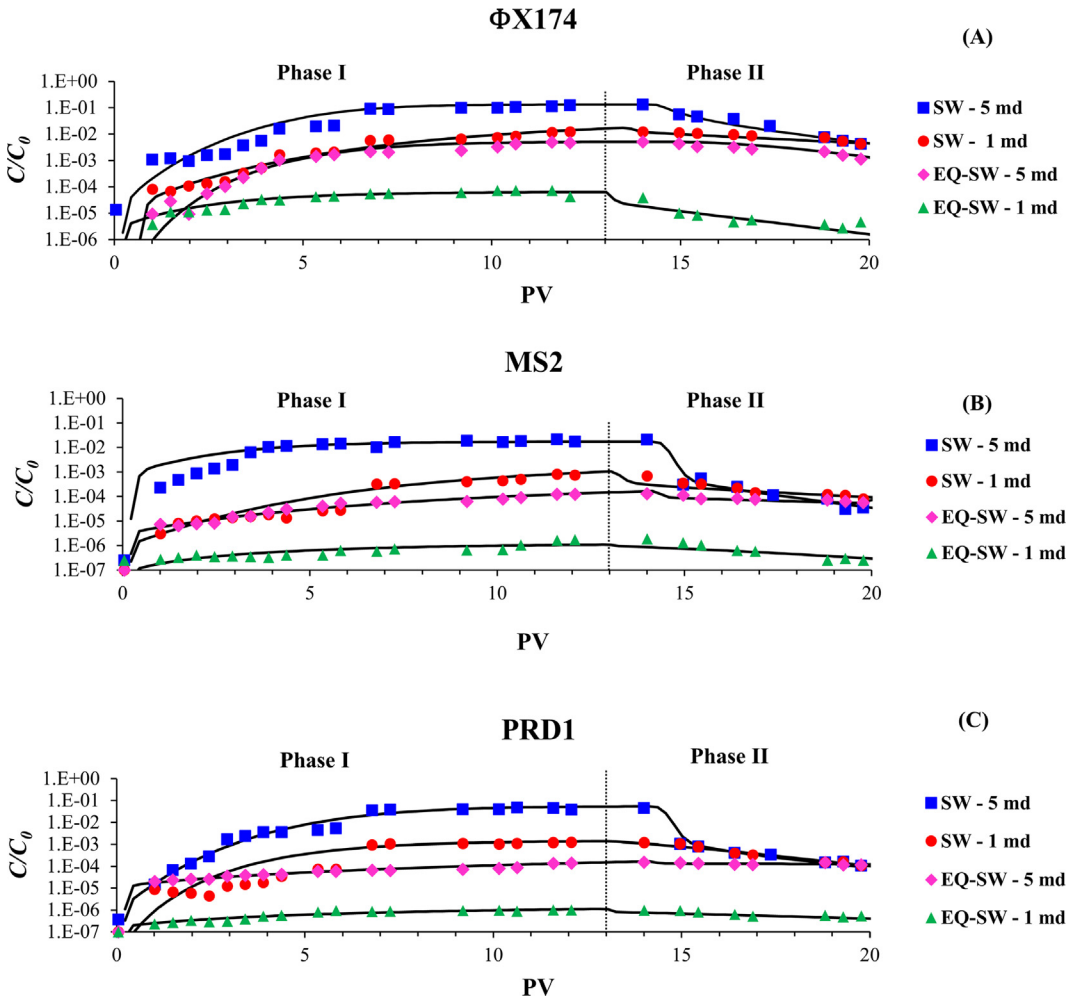

Fig. 1. The observed breakthrough concentrations of viruses **(A)** ΦX174, **(B)** MS2, and **(C)** PRD1 at Phase I (injection of virus in SW or EQ-SW) and the observed effluent concentration in Phase II (injection of virus-free SW or EQ-SW). The Phases I and II were conducted at pore water velocity of 1 or 5 m day^{-1} using either stormwater (SW) or stormwater equilibrated in the aquifer sediment (EQ-SW). Here, the markers are observed data and the solid black line is the fitted model.

Table 2
Experimental conditions and mass balance information from the column experiments. Here, M_{BTC}, $Ms = 100 - M_{BTC}$, $M_{irr} = (100 - M_{BTC} - M_{III} - M_{IV})$, M_{III}, and M_{IV} denote the percentage of the injection MS2, PRD1, and ΦX174 viruses that was recovered in the breakthrough curve, retained on the solid phase, irreversibly retained on the solid phase following the completion of Phases I–IV, and recovered with the injection of Milli-Q water in Phase III and Beef extract with pH 10 in Phase IV, respectively.

Bacteriophage	Velocity [m d^{-1}]	Solution Chemistry	Retention			Release	
			M_{BTC}	M_s	M_{irr}	M_{III}	M_{IV}
			[%]	[%]	[%]	[%]	[%]
ΦX174	1	SW	0.98	99.02	98.37	0.14	0.50
		SW EQ	0.00	100.00	99.94	0.01	0.04
	5	SW	7.70	92.30	91.86	0.06	0.38
		SW EQ	0.35	99.65	99.40	0.01	0.24
MS2	1	SW	0.04	99.96	99.94	0.01	0.01
		SW EQ	0.00	100.00	100.00	0.0001	0.001
	5	SW	1.32	98.68	98.67	0.002	0.006
		SW EQ	0.01	99.99	99.98	0.002	0.009
PRD1	1	SW	0.09	99.91	99.87	0.02	0.02
		SW EQ	0.00	100.00	100.00	0.0002	0.0004
	5	SW	2.51	97.49	97.46	0.01	0.02
		SW EQ	0.01	99.99	99.97	0.001	0.01

experiment. The maximum retention for all three viruses was observed in the experiment conducted under EQ-SW at 1 m day^{-1} (>4.6 logs), whereas the least retention was observed under SW at 5 m day^{-1} (M_s = 92.3%). A detailed discussion of the dependence of virus retention on water velocity, solution chemistry, and virus type is given below.

Fig. 2 indicates that all three viruses always had a higher removal in EQ-SW than SW at a given velocity. Table S1 indicates that the IS and concentration of Ca^{2+} were much higher for EQ-SW than SW. This increase in IS and concentration of Ca^{2+} lowered the magnitude of the zeta potential of the sediment and viruses (Table 1) in EQ-SW and thereby increased the adhesive interaction between the sediment and viruses. Consequently, one key consideration in the determination of virus removal is the effect of ionic strength and the presence of multivalent cations (Harvey and Ryan, 2004). The effects of multivalent cations on virus attachment can be attributed to a number of factors, including the larger ionic radius of Ca^{2+} (1.61 Å) compared to Na^{+} (1.02 Å) (Gutierrez et al., 2010), change in electrostatic interactions between virus and mineral surfaces (Carlson et al. (1968)), cation bridging (Bales et al., 1991; Chu et al., 2003; Pham et al., 2009), charge neutralization (Bales et al., 1991; Lukasik et al., 2000), screening of repulsive surface interaction energies between virus and grain surfaces (McCarthy and McKay, 2004), reduction of the net charge within the electrokinetic shear plane (Simoni et al., 2000), compression of the double-layer (Huysman and Verstraete, 1993), inner sphere complexation of the cations at the virus surfaces (Sadeghi et al., 2013), and the calcium binding to the carboxyl functional groups on the viral protein capsid (Harvey and Ryan, 2004).

Greater removal of viruses occurred at a lower (1 m day^{-1}) than higher (5 m day^{-1}) pore-water velocity under given solution chemistry conditions (Fig. 2). Previous studies have similarly demonstrated that the retention of colloids such as viruses, nanoparticles, and bacteria in porous media is velocity dependent (Hendry et al., 1999; Kim and Lee, 2014; Sasidharan et al., 2017a, 2014; Toloni et al., 2014; Torkzaban et al., 2007). Greater retention of viruses at low flow velocity can be explained by: (i) an increase in the virus residence time (Meinders et al., 1994; Xu et al., 2005); (ii) an increase in the virus adhesive interaction (Xu and Logan, 2006); and (iii) a decrease in the applied hydrodynamic torque that acts on the virus (Bradford et al., 2011; Sasidharan et al., 2017a). It should be mentioned that an increase in residence time increases the time for virus removal. It also increases the probability that viruses can diffuse over shallow energy barriers on physically and chemically heterogeneous surfaces. Consequently, virus removal at a MAR site will be influenced by the flow field, with less removal near the injection well. Careful consideration of the flow field and separation distance between the injection and recovery wells is therefore necessary to achieve the maximum virus removal.

PRD1 is generally considered as the most conservative model for enteric viruses in subsurface viral transport studies (Harvey and Ryan, 2004; Schijven and Hassanizadeh, 2000; Stevenson et al., 2015). In contrast, Fig. 2 indicates that MS2 had the highest removal followed by PRD1 and then by ΦX174 for a given physicochemical condition. Consequently, ΦX174 was the most conservative model virus (had the least removal) in our sediment and stormwater. It is commonly believed that the removal and interactions of viruses with a solid surface are the results of their electrical charge and hydrophobicity (Shields and Farrah, 1987). Table 1 shows that the measured zeta potential values for all three viruses in each solution chemistry were in the same range, so differences in the net zeta potential of the viruses cannot explain these variations in retention. Both PRD1 and MS2 are known to be partially hydrophobic and ΦX174 is hydrophilic in nature (Sasidharan et al., 2016; Schijven and Hassanizadeh, 2000). The presence of some forms of hydrophobic organic matter in the solution (Table S1) and the sediment surface may enhance the hydrophobic interaction between the partially hydrophobic viruses (PRD1 and MS2), which lead to their higher retention. In addition, nanoscale chemical and especially physical heterogeneity on the surfaces of colloids are known to strongly influence their adhesive interaction (Attinti et al., 2010; Bradford et al., 2017). The viral protein coat may contain weakly acidic and basic amino acid groups which act as localized positive and negative charges (Gerba, 1984) and it has a span of hydrophobic amino acids which will determine the hydrophobicity of viruses (Bendersky and Davis, 2011; Bradford and Torkzaban, 2012; Shen, et al., 2012d). The virus surface also contains nanoscale roughness features such as spikes (Huiskonen et al., 2007). Additional research is needed to fully characterize nanoscale variations in chemical heterogeneity and roughness features on the surfaces of our viruses and to assess the influence of these factors on virus retention. Considerable experimental and theoretical research would be needed to address this issue, and it is beyond the scope of this applied study.

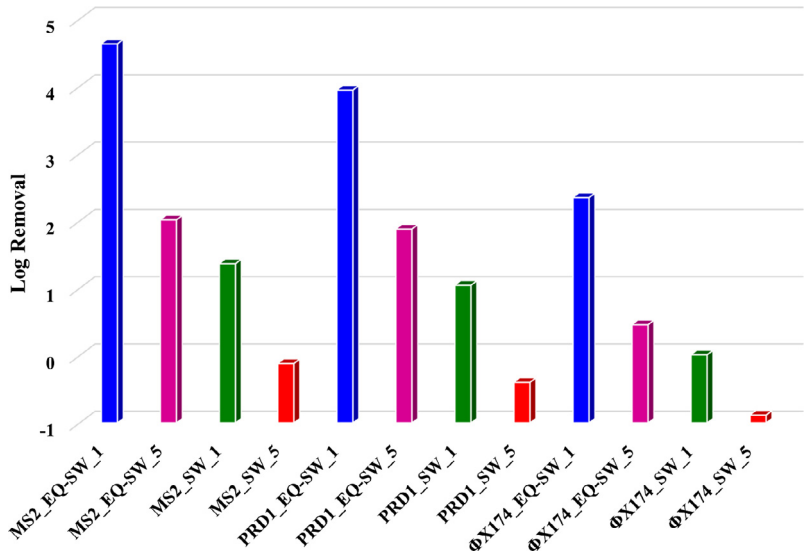

Fig. 2. Bar plots of the log removal (e.g., $-\log_{10}(M_{BTC})$) of viruses under the different physicochemical conditions shown Fig. 1.

3.5. Mathematical modeling of virus retention

Table 3 shows the liquid phase inactivation rate (μ_l) for viruses over the course of the transport and release experiments. The value of μ_l was negligible ($\sim 10^{-7}$ s^{-1}) in both SW or EQ-SW, and was consequently neglected in the mathematical model. A number of different model formulations were employed to describe the virus BTCs. However, low values of the Pearson correlation coefficient (R^2) and nonunique parameter estimates were obtained in many instances. The best model description (R^2 ranged from 67 to 98%) was obtained when considering attachment, detachment, blocking, and a solid phase sink term that accounted for irreversible attachment and inactivation. Straining, clogging, and wedging were not considered as important mechanisms for virus retention in this study, as the ratio of virus to a sediment grain diameter is far below the suggested threshold of 0.003 (Bradford and Bettahar, 2006). Table 4 presents fitted model (k_{att}, k_{det}, S_{max}/C_0, and μ_s) or calculated (α, η, and S_f) parameters, and the R^2 for the goodness of model fit.

Blocking decreases the attachment rate coefficient as available retention sites become filled, and has typically been neglected in most previous virus transport studies (Schijven and Hassanizadeh, 2000). However, Fig. 1 (BTC is plotted in log scale) and Fig. S4 (BTC is plotted in normal scale) indicate that blocking occurred for our viruses and sediment. In particular, BTCs were initially delayed (arriving after 1 PV), next they rapidly increased, and then slowly approached the influent virus concentration. Consistent with our observations, Xu et al. (2017) observed blocking behavior for ΦX174 on a goethite-coated sand. Many others have reported on similar blocking behavior for nanoparticles (Li et al., 2008; Sasidharan et al., 2014; Virkutyte et al., 2014).

Fitted values of S_{max} in the blocking model were subsequently used to determine S_f (Table 4). Calculated values of S_f for the viruses were very small (1.30×10^{-8}–1.45×10^{-4}). Similarly, Xu et al. (2017) reported small values of S_f (0.3×10^{-6}–0.5×10^{-6}) for ΦX174 on a goethite-coated sand. In contrast, values of S_f for 50 and 100 nm latex nanoparticles were much higher on clean quartz sand (0.009–0.39) (Sasidharan et al., 2017b, 2014). Natural solid surfaces like sand grains always contain a wide distribution of physical (e.g., roughness) or chemical (e.g., metal oxides) heterogeneities (Bhattacharjee et al., 1998; Shen et al., 2012c). Previous studies have demonstrated that roughness height and fraction, and positive zeta potential and fraction, at a specific location on the collector (sand) surface can significantly reduce the magnitude of the energy barrier to attachment and the depth of the primary minimum for viruses (Bradford et al., 2017; Bradford and Torkzaban, 2013, 2015; Sasidharan et al., 2017b; Torkzaban and Bradford, 2016). In contrast to smooth latex nanoparticles, the virus exhibits chemical (e.g., lipid membrane and protein coat) (Meder et al., 2013) and physical heterogeneity (e.g., spikes and tail) (Huiskonen et al., 2007; Kazumori, 1981) on their surface. The combination of physical and chemical heterogeneities on both virus and collector surfaces apparently created a shallow primary minimum with negligible energy barrier to attachment and detachment for viruses, and thus, only a very small fraction of the collector surface contributed to S_f.

Previous research has shown that the relative effluent concentration increased and the relative retention decreased with increasing input concentration of colloids as a result of blocking (Leij et al., 2015; Wang et al., 2012). All three viruses were run in the same experiment and had a total input concentration of $\sim 4.9 \times 10^8$ viruses in this study. Conversely, urban stormwater has a much lower enterovirus concentration of 6–170 virus/10 L (Strassler et al., 1999). Consequently, blocking and the subsequent exhaustion of retention sites may not be apparent in some natural systems with low input concentrations. However, recharging stormwater with a high concentration of some forms of organic matter or negatively charged phosphate ions (Table S1) can mask and reverse the charge of positive sites that are favorable for virus retention (Schijven and Hassanizadeh, 2000). This competition for

Table 3
The inactivation rate coefficients (μ_l) of MS2, PRD1, and ΦX174 in the stormwater (SW) and stormwater equilibrated with aquifer sediment (EQ-SW) for the experiment duration (4500 min = 75 h) and the Pearson correlation coefficient (R^2) value calculated using linear regression analysis.

	Solution	μ_l [s^{-1}]	R^2 [%]
ΦX174	SW	8.33×10^{-7}	99.63
	EQ-SW	6.67×10^{-7}	90.98
MS2	SW	5.00×10^{-7}	95.37
	EQ-SW	3.33×10^{-7}	100
PRD1	SW	1.17×10^{-7}	99.78
	EQ-SW	1.00×10^{-7}	100

Table 4
A summary of experimental conditions (solution chemistry and water velocity), model parameters that were fitted to the virus BTCs (the attachment coefficient, k_{att}; the detachment coefficient, k_{det}; the maximum solid phase virus concentration, $\frac{S_{max}}{C_0}$; and a sink term that accounts for irreversible attachment and solid phase inactivation, μ_s) and parameters S_f, α, and η which were calculated from $\frac{S_{max}}{C_0}$, k_{att}, and the correlation equation of Messina et al. (2015), respectively. The table also includes the Pearson correlation coefficient (R^2) for the goodness of model fit, and the standard error values (*S.E.Coeff*) on fitted parameters.

Virus	Solution	Velocity ($m\,day^{-1}$)	R^2 (%)	k_{att} (s^{-1})	*S.E.Coeff* – k_{att}	k_{det} (s^{-1})	*S.E.Coeff* – k_{det}	μ_s (s^{-1})	*S.E.Coeff* – μ_s	S_{max}/C_0 ($cm^3\,gr^{-1}$)	*S.E.Coeff* – S_{max}/C_0	S_f	α	η
MS2	SW	1	94.28	3.25×10^{-3}	9.6×10^{-3}	2.83×10^{-6}	7.8×10^{-5}	1.94×10^{-5}	2.7×10^{-4}	2.11	0.35	1.72×10^{-6}	0.162	0.211
	EQ-SW		67.37	4.26×10^{-3}	1.4×10^{-3}	1.08×10^{-5}	7.6×10^{-4}	3.99×10^{-5}	1.2×10^{-3}	2.49×10^{1}	0.19	2.01×10^{-5}	0.213	0.211
	SW	5	96.81	5.80×10^{-3}	6.1×10^{-2}	2.65×10^{-6}	1.5×10^{-5}	2.32×10^{-4}	3.2×10^{-3}	1.12	0.45	9.12×10^{-7}	0.145	0.085
	EQ-SW		97.21	1.43×10^{-2}	1.7×10^{-2}	1.63×10^{-5}	1.6×10^{-4}	7.14×10^{-5}	7.6×10^{-4}	4.94	0.58	3.99×10^{-6}	0.356	0.085
PRD1	SW	1	79.63	4.86×10^{-3}	5.8×10^{-2}	4.81×10^{-5}	3.2×10^{-3}	5.93×10^{-5}	8.9×10^{-4}	7.77×10^{-1}	0.13	2.74×10^{-6}	0.007	0.127
	EQ-SW		93.53	4.00×10^{-3}	2.4×10^{-3}	3.93×10^{-6}	6.2×10^{-5}	2.11×10^{-5}	1.9×10^{-4}	2.31×10^{1}	0.75	1.45×10^{-4}	0.006	0.127
	SW	5	98.60	1.52×10^{-2}	6.3×10^{-2}	3.95×10^{-6}	8.4×10^{-5}	1.87×10^{-4}	1.7×10^{-3}	7.32×10^{-1}	0.007	2.58×10^{-6}	0.011	0.048
	EQ-SW		96.51	1.21×10^{-2}	1.2×10^{-2}	2.43×10^{-5}	3.2×10^{-4}	4.89×10^{-5}	8.9×10^{-4}	1.53×10^{1}	0.21	9.62×10^{-5}	0.01	0.048
ΦX174	SW	1	96.17	1.18×10^{-3}	2.4×10^{-3}	8.09×10^{-6}	2.2×10^{-4}	1.92×10^{-5}	2.5×10^{-4}	2.24	0.22	4.01×10^{-8}	0.001	0.203
	EQ-SW		96.84	2.86×10^{-3}	6.1×10^{-3}	4.14×10^{-6}	8.9×10^{-5}	4.85×10^{-5}	3.4×10^{-4}	2.17	0.31	5.54×10^{-8}	0.002	0.203
	SW	5	93.55	1.08×10^{-2}	5.8×10^{-3}	1.25×10^{-4}	2.3×10^{-3}	1.86×10^{-4}	1.4×10^{-4}	7.27×10^{-1}	0.003	1.30×10^{-8}	0.005	0.081
	EQ-SW		97.11	3.06×10^{-2}	1.9×10^{-1}	1.08×10^{-3}	1.7×10^{-2}	3.11×10^{-4}	8.6×10^{-4}	1.06	0.12	2.71×10^{-8}	0.013	0.081

the same retention sites and S_{max} could potentially cause blocking to be enhanced.

Colloid filtration theory (CFT) has been developed to predict the value of k_{att} under different physicochemical conditions (Yao et al., 1971). CFT considers that k_{att} is proportional to the product of α and η that account for adhesion and mass transfer, respectively. Consistent with CFT predictions, the value of k_{att} (Table 4) increased with increasing fluid velocity at a given solution chemistry. Similar to Fig. 2, values of k_{att} for MS2 and ΦX174 were always higher for EQ-SW than SW at a given water velocity. However, values of k_{att} for PRD1 were nearly the same for EQ-SW and SW. The observed dependence of k_{att} on the solution chemistry and the virus type was likely complicated by blocking which reduced the apparent value of k_{att}. Both α and S_f are strong functions of the interaction energy between the virus and sediment (Shen et al., 2010; Tufenkji and Elimelech, 2004), so it may not be possible to separately quantify these effects especially when S_f is very low.

The virus BTCs shown in Fig. 1 exhibited low levels of concentration tailing when the columns were eluted with virus-free SW or EQ-SW. The model did not provide an accurate description of this tailing region when k_{det} was considered and μ_s was neglected. Conversely, a good fit was obtained to both the retention and the tailing portion of the BTCs when μ_s and k_{det} (Table 4) were included in the model. Little is known about solid phase inactivation of viruses other than the need for a strong binding force which may disintegrate the protein structure and thereby inhibit the ability of viruses to infect their host (Harvey and Ryan, 2004). Only a few approaches have been developed to separately quantify the rates of virus attachment and solid phase inactivation (Grant et al., 1993; Harvey and Ryan, 2004) such as radiolabeling polio virus capsid and RNA to track the fate of these components (Murray and Parks, 1980). These approaches are difficult, time consuming, and/or require specialized equipment. In this research, these technical challenges were partially overcome through numerical modeling that allows the determination of attachment (k_{att}) and detachment (k_{det}) rates, and a sink term to account for the combined rate of irreversible attachment and solid phase inactivation (μ_s).

Guidelines for MAR have only considered inactivation of viruses in the liquid phase, but have neglected irreversible attachment and solid phase inactivation of viruses (Abu-Ashour et al. (1994); Dillon et al., 2008). Tables 3 and 4 indicate that $k_{att} > \mu_s > k_{det} > \mu_l$, and k_{att} is 3–4 orders of magnitude higher than μ_l. Consequently, guidelines for MAR that only consider liquid phase inactivation will be overly conservative for the considered experimental conditions. Recognizing the removal of viruses via irreversible attachment and/or solid phase inactivation during aquifer storage would help to eliminate some of the expensive post-treatment for recovered MAR water. However, we acknowledge that the virus removal via irreversible attachment and/or solid phase inactivation is highly site specific. Therefore, conducting site specific microbial risk assessment and subsequent development of appropriate MAR design that considers adequate residence time and travel distance based on the horizontal and vertical flow field, soil heterogeneity, and chemical characterization is necessary to achieve the maximum virus removal.

3.6. Release of virus

Fig. 3 shows plots of ΦX174, MS2, and PRD1concentrations in the column effluent during Phases III and IV when Milli-Q water and 3% beef extract with pH = 10 were injected into the column, respectively. Small pulses of released viruses were observed during both phases, with a small peak followed by long concentration tailing. Table 2 summarizes mass balance information from Phases III

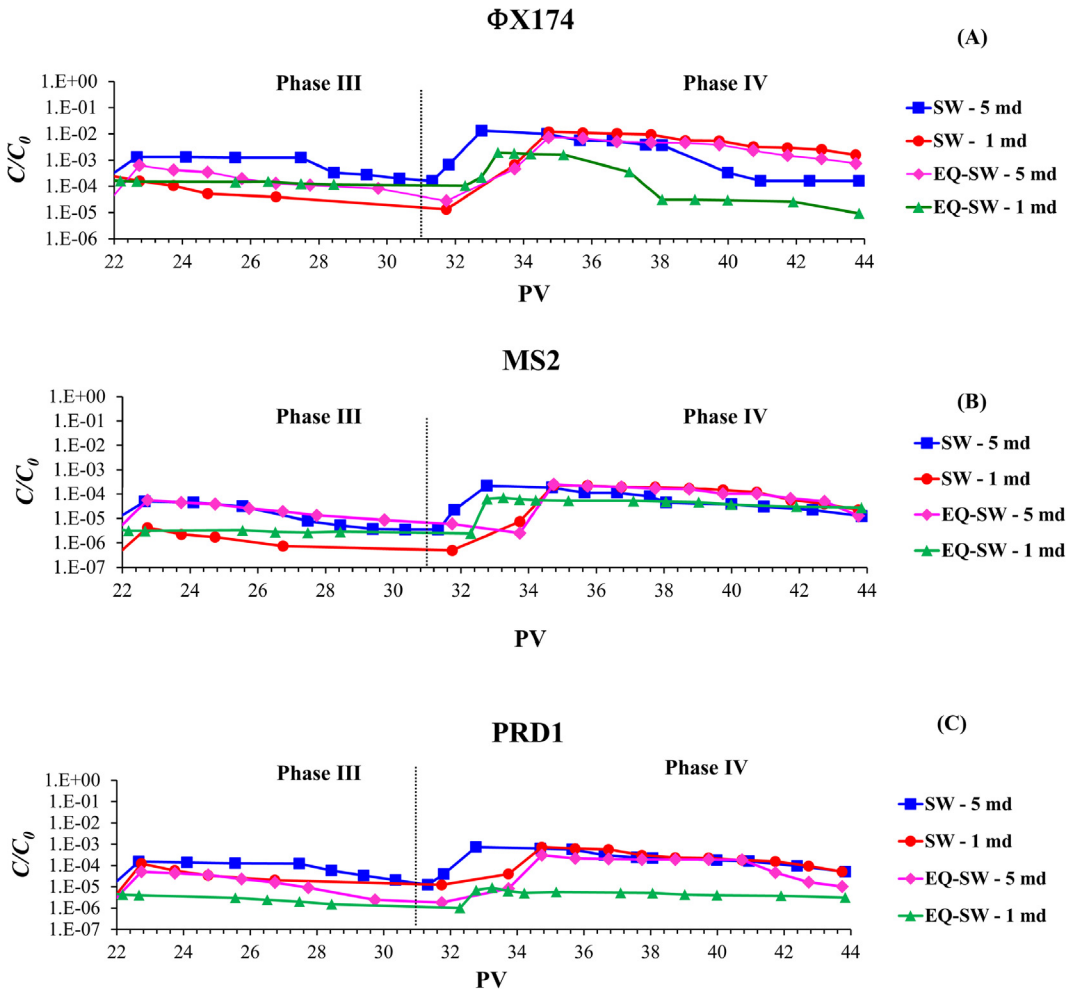

Fig. 3. Observed effluent concentrations of viruses **(A)** ΦX174, **(B)** MS2, and **(C)** PRD1 in Phase III (Milli-Q water) and IV (3% beef extract with pH 10) at a pore-water velocity of 1 and 5 m day^{-1}.

and IV. Only a very small percentage (<0.5%) of the initially attached viruses were released even under the worst-case scenario of beef extract with pH = 10.

Table 2 shows the mass of viruses on the sediment surface that was not recovered after the release Phases III and IV ($M_{irr} = 100 - M_{BTC} - M_{III} - M_{IV}$). The negligible release of viruses and the presence of large $M_{irr} > 91\%$ indicate that the viruses were irreversibly attached or inactivated on the solid surface. Values of M_{irr} followed similar trends to M_s with physicochemical conditions. In particular, M_{irr} was higher for EQ-SW than SW for a given velocity, M_{irr} was higher at lower (1 m day^{-1}) than higher (5 m day^{-1}) pore-water velocity at a given chemistry, and M_{irr} was highest for MS2 followed by PRD1 and then ΦX174. The presence of a large M_s and M_{irr} value for the EQ-SW experiment implies that viruses will irreversibly attach and/or inactivate on the solid before the water reaches the recovery well during an ASTR operation, provided that a sufficient residence time is achieved. An injection event will only release a very tiny fraction of the viruses which may mobilize and re-attach to the surface as the water equilibrates with the sandy limestone aquifer sediment and the IS and the divalent cation concentration increases. Therefore, during ASR operations the chance of releasing the attached viruses during the reverse flow is negligible. However, we assume that the ASTR operation has added advantage of long residence time and travel distance compared to ASR and, therefore, ASTR would be the best option when removal of viruses via attachment/solid phase inactivation is considered.

4. Conclusions and future directions

This research was conducted to better understand and quantify the relative importance of various virus removal processes during MAR in a sandy limestone aquifer. The aquifer sediment was found to remove >92.3% of bacteriophage MS2, PRD1, and ΦX174 from SW and EQ-SW when the pore-water velocity was 1 or 5 m day^{-1}. However, much greater virus removal (4.6 logs) occurred at the lower pore-water velocity and in EQ-SW because of an increase in residence time, IS, and Ca^{2+} concentration. Bacteriophage ΦX174 showed less removal than either PRD1 or especially MS2, and was, therefore, the most conservative model virus for this site. Negligible virus detachment (<0.64%) occurred when columns were flushed with Milli-Q water or beef extract at pH = 10, and this indicates that viruses were irreversibly attached or quickly inactivated on sediment surfaces.

Virus BTCs were successfully simulated using the advection–dispersion equation with terms for attachment, detachment, Langmuirian blocking, and solid phase removal by irreversible attachment and/or surface inactivation. Values of $k_{att} > \mu_s > k_{det} > \mu_l$, and k_{att} was 3–4 orders of magnitude greater than μ_l. The value of k_{det} was always small under steady-state physicochemical conditions. The remaining viruses on the solid phase were either irreversibly retained or inactivated. This process was modeled using the μ_s term. Blocking has commonly been neglected in previous virus transport studies. In contrast, our results clearly demonstrated blocking behavior. The relative importance of blocking is expected

to decrease in a natural setting with lower input concentrations and/or higher S_{max} (Leij et al., 2015). Furthermore, the value of S_f was found to be very small for viruses. This result was attributed to the presence of a shallow primary minimum due to roughness on both the virus and sediment surfaces. Additional research is needed to further assess the potential influence of blocking on virus transport at MAR sites.

MAR has only been considered as a storage option in a water recycling train. Consequently, all previous field scale studies for MAR risk assessments have only considered virus removal by liquid phase inactivation. Current MAR guidelines do not acknowledge the removal of viruses by attachment and solid phase inactivation. This research clearly demonstrated that viruses were irreversibly attached or inactivated on the sediment surface when given enough residence time and that $k_{att} \gg \mu_l$. Natural treatment of injected water during infiltration through the unsaturated zone is widely recognized. However, the mechanisms for natural treatment of virus within the saturated zone is not well understood and the selection of a sub-section of aquifer material with lower carbonate content/higher quartz content represents an environment that is less favorable for virus removal (worst-case scenario). Furthermore, greater virus removal is expected as water moves away from an injection well due to a decrease in water velocity and an increase in IS and Ca^{2+} ions. However, field-scale experiments under actual artificial recharge conditions, using the same bacteriophages employed in this study, showed that the safe setback distance depended on site-specific physicochemical conditions. For example, the setback distance was estimated to be just a few meters (~10 m) in a sandy aquifer in Los Angeles County (Anders and Chrysikopoulos, 2005), whereas the reported setback distance was 8000 ± 4800 m in a fractured aquifer in Southern Italy (Masciopinto et al., 2008). Future MAR guidelines and microbial risk assessment may therefore need to consider site specific removal of viruses by irreversible attachment and solid phase inactivation during the storage period. This could help to eliminate some of the expensive post-treatment to achieve desired water quality.

Notes

The authors declare no competing financial interest.

Acknowledgements

Funding for this research was provided by the National Centre for Groundwater Research and Training (Ph.D. Research Scholarship awarded to S. Sasidharan, 2012–2016), an Australian Government initiative, supported by the Australian Research Council (ARC) and the National Water Commission (NWC). The project was completed in collaboration with CSIRO Land and Water program and the Flinders University of South Australia. The work was conducted in the CSIRO Laboratories at the Waite Campus, Adelaide, South Australia. We acknowledge Ms. Karen Barry (CSIRO, Adelaide) and Mr. John Gouzos (Analytical services unit, CSIRO, Adelaide) for providing assistance in the sediment mineralogy and stormwater chemistry analysis.

Appendix A. Supplementary data

Supplementary data associated with this article can be found, in the online version, at https://doi.org/10.1016/j.jhydrol.2017.10.062.

References

Abu-Ashour, J., Joy, D.M., Lee, H., Whiteley, H.R., Zelin, S., 1994. Transport of microorganisms through soil. Water Air Soil Pollut. 75 (1–2), 141–158.

Adamczyk, Z., Siwek, B., Zembala, M., Belouschek, P., 1994. Kinetics of localized adsorption of colloid particles. Adv. Colloid Interface Sci. 48 (C), 151–280.

Adkinson, A., Watmough, S.A., Dillon, P.J., 2008. Drought-induced metal release from a wetland at Plastic Lake, central Ontario. Can. J. Fish. Aquat. Sci. 65 (5), 834–845. https://doi.org/10.1139/F07-195.

Anders, R., Chrysikopoulos, C.V., 2005. Virus fate and transport during artificial recharge with recycled water. Water Resour. Res. 41 (10). https://doi.org/10.1029/2004WR003419.

Asano, T., Burton, F., Leverenz, H., Tsuchihashi, R., Tchobanoglous, G., 2007. Water reuse: issues, technologies, and applications.

Attinti, R., Wei, J., Kniel, K., Sims, J.T., Jin, Y., 2010. Virus (MS2, 2007. Water Reuse: Issues, Technologies, and Applications. earch, 41(10): DOI:10.1029/2004WR003419Sciences, 65(5): 834-845. DOI:10.1139/F07-195the Australian Research Council (AR1/es903221p

Ayuso-Gabella, N. et al., 2011. Quantifying the effect of Managed Aquifer Recharge on the microbiological human health risks of irrigating crops with recycled water. Agric. Water Manage. 99 (1), 93–102. https://doi.org/10.1016/j.agwat.2011.07.014.

Bales, R.C., Hinkle, S.R., Kroeger, T.W., Stocking, K., Gerba, C.P., 1991. Bacteriophage adsorption during transport through porous media: chemical perturbations and reversibility. Environ. Sci. Technol. 25 (12), 2088–2095.

Bales, R.C., Li, S., Maguire, K.M., Yahya, M.T., Gerba, C.P., 1993. MS-2 and poliovirus transport in porous media: Hydrophobic effects and chemical perturbations. Water Resour. Res. 29 (4), 957–963.

Bekele, E. et al., 2014. Aquifer residence times for recycled water estimated using chemical tracers and the propagation of temperature signals at a managed aquifer recharge site in Australia. Hydrogeol. J. 22 (6), 1383–1401. https://doi.org/10.1007/s10040-014-1142-0.

Bekele, E. et al., 2013. Evaluating two infiltration gallery designs for managed aquifer recharge using secondary treated wastewater. J. Environ. Manage. 117, 115–120. https://doi.org/10.1016/j.jenvman.2012.12.018.

Bekele, E., Toze, S., Patterson, B., Higginson, S., 2011. Managed aquifer recharge of treated wastewater: water quality changes resulting from infiltration through the vadose zone. Water Res. 45 (17), 5764–5772. https://doi.org/10.1016/j.watres.2011.08.058.

Bellou, M.I. et al., 2015. Interaction of human adenoviruses and coliphages with kaolinite and bentonite. Sci. Total Environ. 517, 86–95.

Bendersky, M., Davis, J.M., 2011. DLVO interaction of colloidal particles with topographically and chemically heterogeneous surfaces. J. Colloid Interface Sci. 353 (1), 87–97.

Bergendahl, J., Grasso, D., 2000. Prediction of colloid detachment in a model porous media: hydrodynamics. Chem. Eng. Sci. 55 (9), 1523–1532.

Bhattacharjee, S., Ko, C.H., Elimelech, M., 1998. DLVO interaction between rough surfaces. Langmuir 14 (12), 3365–3375.

Bradford, S.A., Bettahar, M., 2006. Concentration dependent transport of colloids in saturated porous media. J. Contam. Hydrol. 82 (1–2), 99–117. https://doi.org/10.1016/j.jconhyd.2005.09.006.

Bradford, S.A., Kim, H., Shen, C., Sasidharan, S., Shang, J., 2017. Contributions of nanoscale roughness to anomalous colloid retention and stability behavior. Langmuir 33 (38), 10094–10105. https://doi.org/10.1021/acs.langmuir.7b02445.

Bradford, S.A., Torkzaban, S., 2012. Colloid adhesive parameters for chemically heterogeneous porous media. Langmuir 28 (38), 13643–13651. https://doi.org/10.1021/la3029929.

Bradford, S.A., Torkzaban, S., 2013. Colloid interaction energies for physically and chemically heterogeneous porous media. Langmuir 29 (11), 3668–3676. https://doi.org/10.1021/la400229f.

Bradford, S.A., Torkzaban, S., 2015. Determining parameters and mechanisms of colloid retention and release in porous media. Langmuir 31 (44), 12096–12105. https://doi.org/10.1021/acs.langmuir.5b03080.

Bradford, S.A., Torkzaban, S., Wiegmann, A., 2011. Pore-scale simulations to determine the applied hydrodynamic torque and colloid immobilization. Vadose Zone J. 10 (1), 252. https://doi.org/10.2136/vzj2010.0064.

Carlson Jr, G.F., Woodard, F.E., Wentworth, D.F., Sproul, O.J., 1968. Virus inactivation on clay particles in natural waters. J. Water Pollut. Control Fed. 40 (2), R89–R106.

Chen, L., Zhang, G., Wang, L., Wu, W., Ge, J., 2014. Zeta potential of limestone in a large range of salinity. Colloids Surf., A 450, 1–8. https://doi.org/10.1016/j.colsurfa.2014.03.006.

Chrysikopoulos, C.V., Aravantinou, A.F., 2012. Virus inactivation in the presence of quartz sand under static and dynamic batch conditions at different temperatures. J. Hazard. Mater. 233–234, 148–157.

Chu, Y., Jin, Y., Baumann, T., Yates, M.V., 2003. Effect of soil properties on saturated and unsaturated virus transport through columns. J. Environ. Qual. 32 (6), 2017–2025.

Costán-Longares, A. et al., 2008. Microbial indicators and pathogens: removal, relationships and predictive capabilities in water reclamation facilities. Water Res. 42 (17), 4439–4448.

Da Silva, A.K., Kavanagh, O.V., Estes, M.K., Elimelech, M., 2011. Adsorption and aggregation properties of norovirus GI and GII virus-like particles demonstrate differing responses to solution chemistry. Environ. Sci. Technol. 45 (2), 520–526. https://doi.org/10.1021/es102368d.

Dillon, P. et al., 2008. A critical evaluation of combined engineered and aquifer treatment systems in water recycling. Water Sci. Technol. 57 (5), 753–762.

Dillon, P., Pavelic, P., Page, D., Beringen, H., Ward, J., 2009. Managed Aquifer Recharge: An Introduction. CSIRO, National Water Commission.

Donald, M., Mengersen, K., Toze, S., Sidhu, J.P.S., Cook, A., 2011. Incorporating parameter uncertainty into quantitative microbial risk assessment (QMRA). J. Water Health 9 (1), 10–26. https://doi.org/10.2166/wh.2010.073.
Earle, S., 2013. Groundwater Geochemistry. Vancouver Island University, Canada.
Elimelech, M., 1994. Effect of particle size on the kinetics of particle deposition under attractive double layer interactions. J. Colloid Interface Sci. 164 (1), 190–199. https://doi.org/10.1006/jcis.1994.1157.
Elimelech, M., Chen, W.H., Waypa, J.J., 1994. Measuring the zeta (electrokinetic) potential of reverse osmosis membranes by a streaming potential analyzer. Desalination 95 (3), 269–286.
Foppen, J.W.A., Okletey, S., Schijven, J.F., 2006. Effect of goethite coating and humic acid on the transport of bacteriophage PRD1 in columns of saturated sand. J. Contam. Hydrol. 85 (3–4), 287–301. https://doi.org/10.1016/j.jconhyd.2006.02.004.
Gerba, C.P., 1983. Virus survival and transport in groundwater. Developments in Industrial Microbiology (USA).
Gerba, C.P., 1984. Applied and theoretical aspects of virus adsorption to surfaces. Adv. Appl. Microbiol. 30, 133–168. https://doi.org/10.1016/s0065-2164(08)70054-6.
Grant, S.B., List, E.J., Lidstrom, M.E., 1993. Kinetic analysis of virus adsorption and inactivation in batch experiments. Water Resour. Res. 29 (7), 2067–2085.
Gutierrez, L., Mylon, S.E., Nash, B., Nguyen, T.H., 2010. Deposition and aggregation kinetics of rotavirus in divalent cation solutions. Environ. Sci. Technol. 44 (12), 4552–4557.
Harvey, R.W., Ryan, J.N., 2004. Use of PRD1 bacteriophage in groundwater viral transport, inactivation, and attachment studies. FEMS Microbiol. Ecol. 49 (1), 3–16. https://doi.org/10.1016/j.femsec.2003.09.015.
Hendry, M.J., Lawrence, J.R., Maloszewski, P., 1999. Effects of velocity on the transport of two bacteria through saturated sand. Ground Water 37 (1), 103–112.
Hijnen, W.A., Brouwer-Hanzens, A.J., Charles, K.J., Medema, G.J., 2005. Transport of MS2 phage, Escherichia coli, *Clostridium perfringens*, *Cryptosporidium parvum*, and *Giardia intestinalis* in a gravel and a sandy soil. Environ. Sci. Technol. Lett. 39 (20), 7860–7868.
Huiskonen, J.T., Manole, V., Butcher, S.J., 2007. Tale of two spikes in bacteriophage PRD1. Proc. Natl. Acad. Sci. 104 (16), 6666–6671.
Huysman, F., Verstraete, W., 1993. Effect of cell surface characteristics on the adhesion of bacteria to soil particles. Biol. Fertil. Soils 16 (1), 21–26. https://doi.org/10.1007/bf00336510.
Johnson, P.R., Elimelech, M., 1995. Dynamics of colloid deposition in porous media: Blocking based on random sequential adsorption. Langmuir 11 (3), 801–812.
Karageorgiou, K., Paschalis, M., Anastassakis, G.N., 2007. Removal of phosphate species from solution by adsorption onto calcite used as natural adsorbent. J. Hazard. Mater. 139 (3), 447–452. https://doi.org/10.1016/j.jhazmat.2006.02.038.
Kazumori, Y., 1981. Electron microscopic studies of bacteriophage φ X174 intact and 'eclipsing'particles, and the genome by the staining and shadowing method. J. Virol. Methods 2 (3), 159–167.
Kim, C., Lee, S., 2014. Effect of seepage velocity on the attachment efficiency of TiO2 nanoparticles in porous media. J. Hazard. Mater. 279, 163–168. https://doi.org/10.1016/j.jhazmat.2014.06.072.
Kim, H.N., Bradford, S.A., Walker, S.L., 2009. Escherichia coli O157: H7 transport in saturated porous media: role of solution chemistry and surface macromolecules. Environ. Sci. Technol. 43 (12), 4340–4347. https://doi.org/10.1021/es8026055.
Knappett, P.S., Emelko, M.B., Zhuang, J., McKay, L.D., 2008. Transport and retention of a bacteriophage and microspheres in saturated, angular porous media: effects of ionic strength and grain size. Water Res. 42 (16), 4368–4378. https://doi.org/10.1016/j.watres.2008.07.041.
Kremer, S., Pavelic, P., Dillon, P., Barry, K., 2008. Flow and solute transport observations and modeling from the first phase of flushing operations at the Salisbury ASTR Site. Water for a Healthy Country National Research Flagship.
Landry, E., Vaughn, J., Thomas, M., Vicale, T., 1978. Efficiency of beef extract for the recovery of poliovirus from wastewater effluents. Appl. Environ. Microbiol. 36 (4), 544–548.
Leij, F.J., Bradford, S.A., Wang, Y., Sciortino, A., 2015. Langmuirian blocking of irreversible colloid retention: analytical solution, moments, and setback distance. J. Environ. Qual. 44 (5). https://doi.org/10.2134/jeq2015.03.0147.
Levantesi, C. et al., 2010. Quantification of pathogenic microorganisms and microbial indicators in three wastewater reclamation and managed aquifer recharge facilities in Europe. Sci. Total Environ. 408 (21), 4923–4930. https://doi.org/10.1016/j.scitotenv.2010.07.042.
Li, Y., Wang, Y., Pennell, K.D., Briola, L.M.A., 2008. Investigation of the transport and deposition of fullerene (C60) nanoparticles in quartz sands under varying flow conditions. Environ. Sci. Technol. 42 (19), 7174–7180.
Lin, E. et al., 2006. Evaluation of Roughing Filtration for Pre-treatment of Stormwater Prior to Aquifer Storage Recovery (ASR). CSIRO Land and Water.
Lipson, S.M., Stotzky, G., 1983. Adsorption of reovirus to clay minerals: effects of cation-exchange capacity, cation saturation, and surface area. Appl. Environ. Microbiol. 46 (3), 673–682.
Loveland, J.P., Ryan, J.N., Amy, G.L., Harvey, R.W., 1996. The reversibility of virus attachment to mineral surfaces. Colloids Surf., A 107, 205–221.
Lukasik, J., Scott, T.M., Andryshak, D., Farrah, S.R., 2000. Influence of salts on virus adsorption to microporous filters. Appl. Environ. Microbiol. 66 (7), 2914–2920. https://doi.org/10.1128/AEM.66.7.2914-2920.2000.
Malvern Instruments Ltd, 2004. Zetasizer Nano Series User Manual. Malvern Instruments Ltd, United Kingdom.
Masciopinto, C., La Mantia, R., Chrysikopoulos, C.V., 2008. Fate and transport of pathogens in a fractured aquifer in the Salento area, Italy. Water Resour. Res. 44 (1).
Mayotte, J.-M., Hölting, L., Bishop, K., 2017. Reduced removal of bacteriophage MS2 in during basin infiltration managed aquifer recharge as basin sand is exposed to infiltration water. Hydrol. Process. 31 (9), 1690–1701. https://doi.org/10.1002/hyp.11137.
McCarthy, J.F., McKay, L.D., 2004. Colloid transport in the subsurface: Past, present, and future challenges. Vadose Zone J. 3 (2), 326–337.
McMinn, B.R., 2013. Optimization of adenovirus 40 and 41 recovery from tap water using small disk filters. J. Virol. Methods 193 (2), 284–290. https://doi.org/10.1016/j.jviromet.2013.06.021.
Meder, F. et al., 2013. The role of surface functionalization of colloidal alumina particles on their controlled interactions with viruses. Biomaterials 34 (17), 4203–4213.
Meinders, J.M., van der Mei, H.C., Busscher, H.J., 1994. Physicochemical aspects of deposition of Streptococcus thermophilus b to hydrophobic and hydrophilic substrata in a parallel plate flow chamber. J. Colloid Interface Sci. 164 (2), 355–363. https://doi.org/10.1006/jcis.1994.1177.
MelbourneWater, Treatment train. Melbourne Water, Melbourne, 2017. https://www.melbournewater.com.au/planning-and-building/stormwater-management/options-treating-stormwater/treatment-train [Accessed on August 2017].
Messina, F., Marchisio, D.L., Sethi, R., 2015. An extended and total flux normalized correlation equation for predicting single-collector efficiency. J. Colloid Interface Sci. 446, 185–193. https://doi.org/10.1016/j.jcis.2015.01.024.
Miotliński, K., Dillon, P.J., Pavelic, P., Barry, K., Kremer, S., 2014. Recovery of injected freshwater from a brackish aquifer with a multiwell system. Groundwater 52 (4), 495–502.
Moore, R.S., Taylor, D.H., Sturman, L.S., Reddy, M.M., Fuhs, G.W., 1981. Poliovirus adsorption by 34 minerals and soils. Appl. Environ. Microbiol. 42 (6), 963–975.
Murray, J.P., Laband, S.J., 1979. Degradation of poliovirus by adsorption on inorganic surfaces. Appl. Environ. Microbiol. 37 (3), 480–486.
Murray, J.P., Parks, G.A., 1980. Poliovirus adsorption on oxide surfaces, particulates in water. Adv. Chem., 97–133
Page, D., Dillon, P., Toze, S., Sidhu, J.P.S., 2010a. Characterising aquifer treatment for pathogens in managed aquifer recharge. Water Sci. Technol. 62 (9), 2009–2015. https://doi.org/10.2166/wst.2010.539.
Page, D. et al., 2010b. Risk assessment of aquifer storage transfer and recovery with urban stormwater for producing water of a potable quality. J. Environ. Qual. 39 (6), 2029–2039. https://doi.org/10.2134/jeq2010.0078.
Page, D., Dillon, P., Toze, S., Bixio, D., Genthe, B., Cisneros, B.E.J., Wintgens, T., 2010c. Valuing the subsurface pathogen treatment barrier in water recycling via aquifers for drinking supplies. Water Res. 44 (6), 1841–1852.
Page, D. et al., 2015a. Assessment of treatment options of recycling urban stormwater recycling via aquifers to produce drinking water quality. Urban Water J. 1–6. https://doi.org/10.1080/1573062X.2015.1024691.
Page, D. et al., 2015b. E. coli and turbidity attenuation during urban stormwater recycling via aquifer storage and recovery in a brackish limestone aquifer. Ecol. Eng. 84, 427–434.
Panthi, S., 2003. Carbonate chemistry and calcium carbonate saturation state of rural water supply projects in Nepal. In: Proceedings of the Seventh International Water Technology Conference, Cairo, Egypt, pp. 1–3.
Pavelic, P., Dillon, P.J., Robinson, N., 2004. Groundwater Modeling to Assist Well-Field Design and Operation for the ASTR Trial at Salisbury. Citeseer, South Australia.
Pham, M., Mintz, E.A., Nguyen, T.H., 2009. Deposition kinetics of bacteriophage MS2 to natural organic matter: role of divalent cations. J. Colloid Interface Sci. 338 (1), 1–9. https://doi.org/10.1016/j.jcis.2009.06.025.
Radke, B., Watkins, K.L., Bauld, J., 1998. A Groundwater Quality Assessment of Shallow Aquifers in the Darwin Rural Area, Northern Territory, 1. Australian Geological Survey Organisation.
Redman, J.A. et al., 1999. Physicochemical mechanisms responsible for the filtration and mobilization of a filamentous bacteriophage in quartz sand. Water Res. 33 (1), 43–52. https://doi.org/10.1016/S0043-1354(98)00194-8.
Rinck-Pfeiffer, S., Pitman, C., Dillon, P., 2005. Stormwater ASR in practice and ASTR (aquifer storage transfer and recovery) under investigation in Salisbury, South Australia. In: Proc. Fifth International Symposium on Management of Aquifer Recharge, United Nations Educational, Scientific, and Cultural Organization, IHP-VI, Series of Groundwater, Berlin.
Roy, S.B., Dzombak, D.A., 1996. Na+-Ca2+ exchange effects in the detachment of latex colloids deposited in glass bead porous media. Colloids Surf., A 119 (2–3), 133–139.
Ryan, J.N. et al., 2002. Field and laboratory investigations of inactivation of viruses (PRD1 and MS2) attached to iron oxide-coated quartz sand. Environ. Sci. Technol. 36 (11), 2403–2413.
Sadeghi, G., Behrends, T., Schijven, J.F., Hassanizadeh, S.M., 2013. Effect of dissolved calcium on the removal of bacteriophage PRD1 during soil passage: the role of double-layer interactions. J. Contam. Hydrol. 144 (1), 78–87. https://doi.org/10.1016/j.jconhyd.2012.10.006.
Sasidharan, S. et al., 2017a. Unraveling the complexities of the velocity dependency of *E. coli* retention and release parameters in saturated porous media. Sci. Total Environ. 603–604, 406–415. https://doi.org/10.1016/j.scitotenv.2017.06.091.
Sasidharan, S., Torkzaban, S., Bradford, S.A., Cook, P.G., Gupta, V.V., 2017b. Temperature dependency of virus and nanoparticle transport and retention in

saturated porous media. J. Contam. Hydrol. 196, 10–20. https://doi.org/10.1016/j.jconhyd.2016.11.004.
Sasidharan, S., Torkzaban, S., Bradford, S.A., Dillon, P.J., Cook, P.G., 2014. Coupled effects of hydrodynamic and solution chemistry on long-term nanoparticle transport and deposition in saturated porous media. Colloids Surf., A 457, 169–179. https://doi.org/10.1016/j.colsurfa.2014.05.075.
Sasidharan, S. et al., 2016. Transport and retention of bacteria and viruses in biochar-amended sand. Sci. Total Environ. 548–549, 100–109. https://doi.org/10.1016/j.scitotenv.2015.12.126.
Schijven, J., Berger, Philip, Miettinen, Ilkka, 2003. Removal of Pathogens, Surrogates, Indicators, and Toxins Using Riverbank Filtration. Riverbank Filteration. Springer, Netherlands, pp. 73–116.
Schijven, J.F., Hassanizadeh, S.M., 2000. Removal of viruses by soil passage: Overview of modeling, processes, and parameters. Crit. Rev. Environ. Sci. Technol. 30 (1), 49–127.
Shannon, M.A. et al., 2008. Science and technology for water purification in the coming decades. Nature 452 (7185), 301–310.
Shen, C., Huang, Y., Li, B., Jin, Y., 2010. Predicting attachment efficiency of colloid deposition under unfavorable attachment conditions. Water Resour. Res. 46 (11). https://doi.org/10.1029/2010wr009218.
Shen, C. et al., 2012a. Coupled factors influencing detachment of nano- and micro-sized particles from primary minima. J. Contam. Hydrol. 134–135, 1–11. https://doi.org/10.1016/j.jconhyd.2012.04.003.
Shen, C. et al., 2012b. Theoretical and experimental investigation of detachment of colloids from rough collector surfaces. Colloids Surf., A 410, 98–110. https://doi.org/10.1016/j.colsurfa.2012.06.025.
Shen, C. et al., 2012c. Application of DLVO energy map to evaluate interactions between spherical colloids and rough surfaces. Langmuir 28 (41), 14681–14692. https://doi.org/10.1021/la303163c.
Shen, C., Wang, L.-P., Li, B., Huang, Y., Jin, Y., 2012d. Role of surface roughness in chemical detachment of colloids deposited at primary energy minima. Vadose Zone J. 11 (1). https://doi.org/10.2136/vzj2011.0057.
Shields, P., Farrah, S., 1987. Determination of the electrostatic and hydrophobic character of enteroviruses and bacteriophages. In: 87th Annual Meeting American Society of Microbiology. American Society of Microbiology, Washington DC.
Sidhu, J. et al., 2015. Pathogen decay during managed aquifer recharge at four sites with different geochemical characteristics and recharge water sources. J. Environ. Qual. 44 (5), 1402–1412.
Sidhu, J.P.S., Toze, S., 2012. Assessment of pathogen survival potential during managed aquifer recharge with diffusion chambers. J. Appl. Microbiol. 113 (3), 693–700. https://doi.org/10.1111/j.1365-2672.2012.05360.x.
Sikora, A., Shard, A.G., Minelli, C., 2016. Size and zeta-potential measurement of silica nanoparticles in serum using tunable resistive pulse sensing. Langmuir 32 (9), 2216–2224. https://doi.org/10.1021/acs.langmuir.5b04160.
Simoni, S.F., Bosma, T.N.P., Harms, H., Zehnder, A.J.B., 2000. Bivalent cations increase both the subpopulation of adhering bacteria and their adhesion efficiency in sand columns. Environ. Sci. Technol. 34 (6), 1011–1017. https://doi.org/10.1021/es990476m.
Šimůnek, J., van Genuchten, M.T., Šejna, M., 2016. Recent developments and applications of the HYDRUS computer software packages. Vadose Zone J. 15 (7).
Stevens, D., 2014. Managed aquifer recharge and stormwater use options: Audit of the Parafield stormwater harvesting and managed aquifer recharge system for non-potable use against the stormwater risk-based management plan, Goyder Institute for Water Research.
Stevenson, M.E. et al., 2015. Attachment and detachment behavior of human Adenovirus and surrogates in fine granular limestone aquifer material. J. Environ. Qual. 44 (5), 1392–1401.
Strassler, E., Pritts, J., Strellec, K., 1999. Preliminary data summary of urban stormwater best management practices. The United States Environmental Protection Agency, Office of Water.
Sverdrup, H., Warfvinge, P., 1993. Calculating field weathering rates using a mechanistic geochemical model PROFILE. Appl. Geochem. 8 (3), 273–283. https://doi.org/10.1016/0883-2927(93)90042-F.
Thomson, N.R., 2005. Bringing groundwater quality research to the watershed scale. In: IAHS Proceedings & Reports. International Association of Hydrological Sciences, UK, 576 pp.
Toloni, I., Lehmann, F., Ackerer, P., 2014. Modeling the effects of water velocity on TiO2 nanoparticles transport in saturated porous media. J. Contam. Hydrol. 171, 42–48.
Tombácz, E., 2009. pH-dependent surface charging of metal oxides. Periodica polytechnica. Chem. Eng. 53 (2), 77.
Torkzaban, S., Bradford, S.A., 2016. Critical role of surface roughness on colloid retention and release in porous media. Water Res. 88, 274–284. https://doi.org/10.1016/j.watres.2015.10.022.
Torkzaban, S., Bradford, S.A., Walker, S.L., 2007. Resolving the coupled effects of hydrodynamics and DLVO forces on colloid attachment in porous media. Langmuir 23 (19), 9652–9660. https://doi.org/10.1021/la700995e.
Toze, S., Bekele, E., 2009. Managed aquifer recharge with secondary treated wastewater. Water 36 (2), 43–47.
Toze, S., Bekele, E., Page, D., Sidhu, J., Shackleton, M., 2010. Use of static quantitative microbial risk assessment to determine pathogen risks in an unconfined carbonate aquifer used for managed aquifer recharge. Water Res. 44 (4), 1038–1049. https://doi.org/10.1016/j.watres.2009.08.028.
Tufenkji, N., Elimelech, M., 2004. Correlation equation for predicting single-collector efficiency in physicochemical filtration in saturated porous media. Environ. Sci. Technol. 38 (2), 529–536.
UN, 2013. Water Scarcity factsheet. In: Affairs, U.N.D.o.E.a.S. (Ed.). United Nations Department of Economic and Social Affairs, United Nations. http://www.unwater.org/ [Accessed June 2017].
Vanderzalm, J.L., Page, D.W., Barry, K.E., Dillon, P.J., 2010. A comparison of the geochemical response to different managed aquifer recharge operations for injection of urban stormwater in a carbonate aquifer. Appl. Geochem. 25 (9), 1350–1360. https://doi.org/10.1016/j.apgeochem.2010.06.005.
Vega, E., Lesikar, B., Pillai, S.D., 2003. Transport and survival of bacterial and viral tracers through submerged-flow constructed wetland and sand-filter system. Bioresour. Technol. 89 (1), 49–56.
Virkutyte, J., Al-Abed, S.R., Choi, H., Bennett-Stamper, C., 2014. Distinct structural behavior and transport of TiO2 nano- and nanostructured particles in sand. Colloids Surf., A 443, 188–194.
Wade, A., 1992. Problem constituents in Australian groundwater drinking-water supplies. BMR J. Aust. Geol. Geophys. BJAGDT 13 (1).
Walshe, G.E., Pang, L., Flury, M., Close, M.E., Flintoft, M., 2010. Effects of pH, ionic strength, dissolved organic matter, and flow rate on the co-transport of MS2 bacteriophages with kaolinite in gravel aquifer media. Water Res. 44 (4), 1255–1269.
Wang, C. et al., 2012. Retention and transport of silica nanoparticles in saturated porous media: effect of concentration and particle size. Environ. Sci. Technol. 46 (13), 7151–7158. https://doi.org/10.1021/es300314n.
Ward, J., Dillon, P., 2009. Robust design of managed aquifer recharge policy in Australia. Water for a Healthy Country Flagship Report to National Water Commission.
Ward, R.L. et al., 1986. Human rotavirus studies in volunteers: determination of infectious dose and serological response to infection. J. Infect. Dis. 154 (5), 871–880.
Xu, L.-C., Logan, B.E., 2006. Adhesion forces between functionalized latex microspheres and protein-coated surfaces evaluated using colloid probe atomic force microscopy. Colloids Surf., B 48 (1), 84–94.
Xu, L.C., Vadillo-Rodriguez, V., Logan, B.E., 2005. Residence time, loading force, pH, and ionic strength affect adhesion forces between colloids and biopolymer-coated surfaces. Langmuir 21 (16), 7491–7500.
Xu, S. et al., 2017. Mutually facilitated co-transport of two different viruses through reactive porous media. Water Res. 123, 40–48. https://doi.org/10.1016/j.watres.2017.06.039.
Yao, K.-M., Habibian, M.T., O'Melia, C.R., 1971. Water and wastewater filtration. Concepts and applications. Environ. Sci. Technol. 5 (11), 1105–1112. https://doi.org/10.1021/es60058a005.
Yates, M.V., Gerba, C.P., Kelley, L.M., 1985. Virus persistence in groundwater. Appl. Environ. Microbiol. 49 (4), 778–781.
Yates, M.V., Yates, S.R., Gerba, C.P., 1988. Modeling microbial fate in the subsurface environment. Crit. Rev. Environ. Sci. Technol. 17 (4), 307–344.
Yates, M.V., Yates, S.R., Wagner, J., Gerba, C.P., 1987. Modeling virus survival and transport in the subsurface. J. Contam. Hydrol. 1 (3), 329–345.
Zhuang, J., Jin, Y., 2003. Virus retention and transport as influenced by different forms of soil organic matter. J. Environ. Qual. 32 (3), 816–823.